THE BELL SYSTEM TECHNICAL JOURNAL
Vol. 54, No. 7, September 1975
Printed in U.S.A.

Some Far-Field Studies of an Offset Launcher

By M. J. GANS and R. A. SEMPLAK

(Manuscript received January 24, 1975)

An offset paraboloidal reflector illuminated by a balanced feed horn constitutes an efficient launcher for coupling microwaves into quasi-optical beams. Measurements on a launcher with low blockage show low cross polarization. The amplitude, phase, and polarization characteristics are predicted by two gaussian beam modes, and the resulting formulas are found to agree well with measurements at 19 and 28 GHz. For example, with increasing offset angles, the ratio of the maximum cross-polarized signal in the radiation pattern to the on-axis co-polarized signal is observed to vary from −44 to −37 dB, within 1 dB of the predicted variation.

I. INTRODUCTION

At millimeter wavelengths, normal waveguide losses become too large in many applications; for example, long lengths of waveguide are required in satellite earth stations between the transceiver and the reflector antenna focus. To reduce these losses, one may use quasi-optical beams that employ reflectors or lenses for refocussing at various intervals, thereby confining the beam within a geometric tube with no (lossy) guiding walls. To couple the circuit components to these beams, it is desirable to provide a beam launcher that has quasi-gaussian amplitude over the aperture, low loss, good polarization purity, and high return loss.

Offset reflectors provide high return loss, i.e., they are well matched, because the radiation field of the illuminated aperture bypasses and, therefore, does not reenter the feed horn.[1] If the reflector is made large so that the level of the feed-horn illumination at the edge of the reflector is low, spillover and diffraction losses are small. Also, since the feed horn does not block the aperture of the reflector, blockage losses are negligible, and the radiation patterns are unaffected. But cross polarization can be serious with offset reflectors, as pointed out in Ref. 2; however, by choosing a small offset angle the cross polarization can be held to acceptable levels throughout the beam.

Here, the far-field properties of an offset paraboloidal reflector (Fig. 1) are investigated. Section II describes the radiation charac-

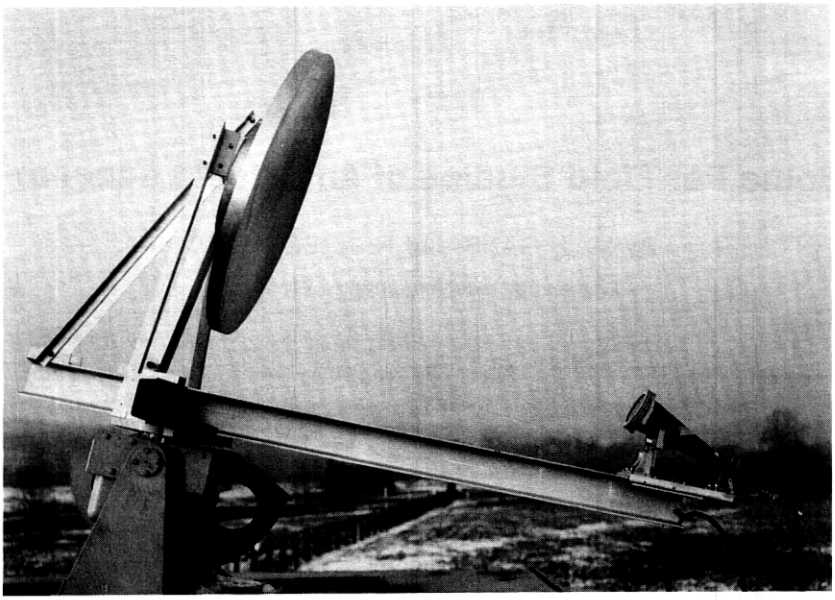

Fig. 1—Offset launcher. The 76-cm (30-in.) diameter reflector is a numerically machined section of a paraboloid. Reflector focal length is 115.7 cm and it is fed, in this instance, by a 28.5-GHz dual-mode horn with a polarizer.

teristics of the dual-mode feed horns, the experimental setups, and the measurements of the far-field properties of the complete launcher. Section III provides the theoretical formulas showing that the radiation performance of offset launchers can be well characterized in terms of gaussian modes.

Specific applications of this type of launcher are in feeding Cassegrainian antennas of the type discussed in Ref. 1, and in launching and collecting beams on Hertzian cable transmission lines.[3]

II. MEASUREMENTS

2.1 Dual-mode feed horns

The dual-mode feed horn designed to feed the offset launcher of Fig. 1 is shown in Fig. 2a. The input section generates the TE_{11} and TM_{11} modes in a circular waveguide by means of a conical step in the waveguide.[4] This section slides in the input waveguide so that the length from the step to the horn aperture, the "drift space," may be adjusted to co-phase the TE_{11} and TM_{11} modes to provide zero current at the edge of the aperture (minimizing the side lobes and symmetrizing the pattern). The small horn taper angle of 7.121 degrees was chosen to prevent disturbing the TE_{11} and TM_{11} modes, and to provide a

FREQUENCY, F IN GHz	DIAMETER, D IN cm	LENGTH, L IN cm
19.04	12.70	59.06
28.56	8.38	39.37

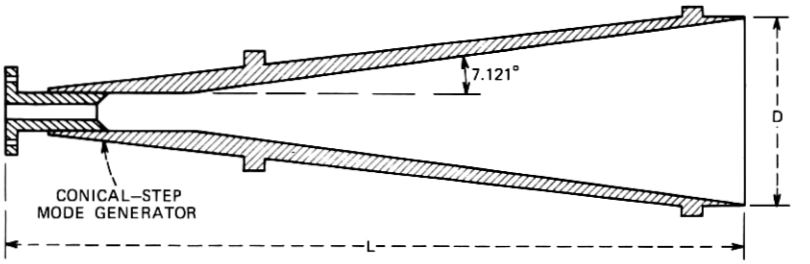

(a)

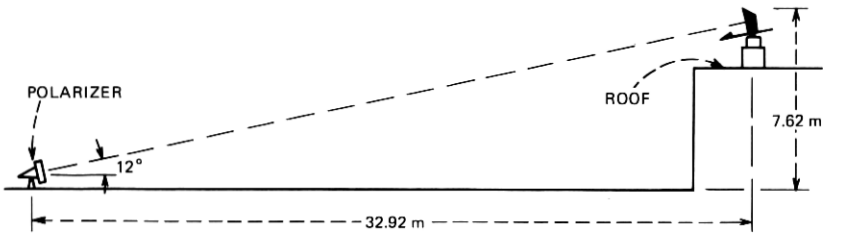

(b)

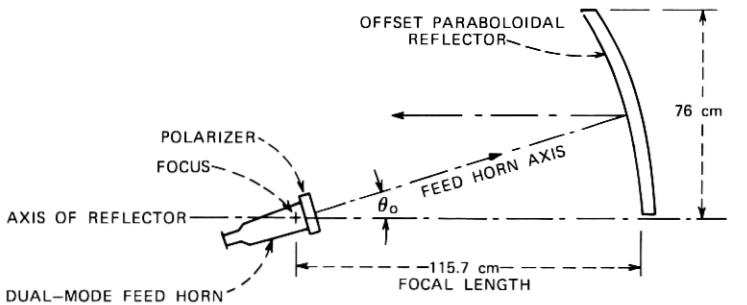

(c)

Fig. 2—(a) Cross-sectional view of the dual-mode feed-horn design used for the offset launcher of Fig. 1. (b) Profile of measuring range. (c) Launcher schematic.

small aperture phase error [$\epsilon = (2\pi/\lambda)(D^2/8L) = \pi/2$ radians] without making the horn too long.

The azimuth radiation patterns of 28.5-GHz dual-mode feed horns for horizontal, vertical, and 45-degree polarizations, along with the associated cross polarizations for each case, as measured in an anechoic chamber, are shown in Fig. 3. Figure 3a shows the results obtained

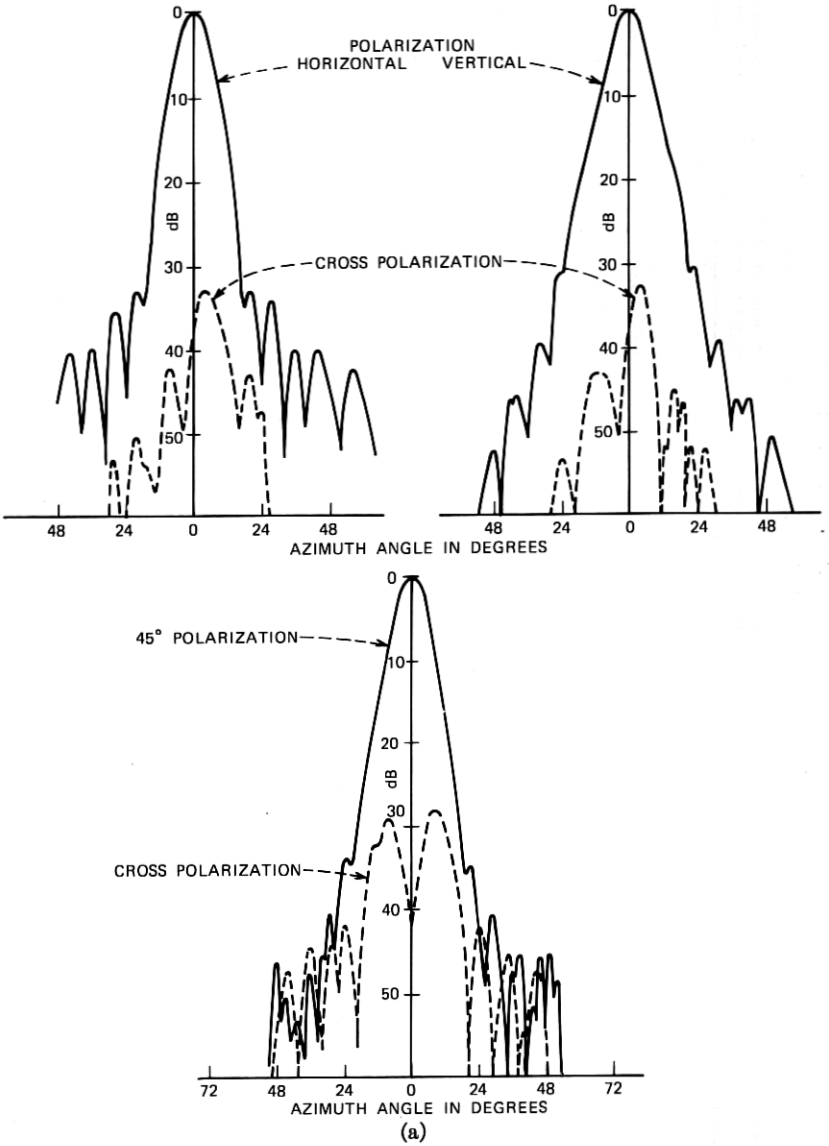

Fig. 3—The 28.5-GHz dual-mode feed-horn radiation patterns for the principal and 45-degree polarizations. Included are the corresponding cross polarizations: (a) without polarizer on dual-mode feed; (b) with polarizer on dual-mode feed.

without a polarizer on a horn. Note that the cross polarization for the 45-degree polarization condition has peaks of about −28 dB at angles of about ±8 degrees. (This behavior of dual-mode horns is predictable; superior cross-polarization performance is obtainable from hybrid-

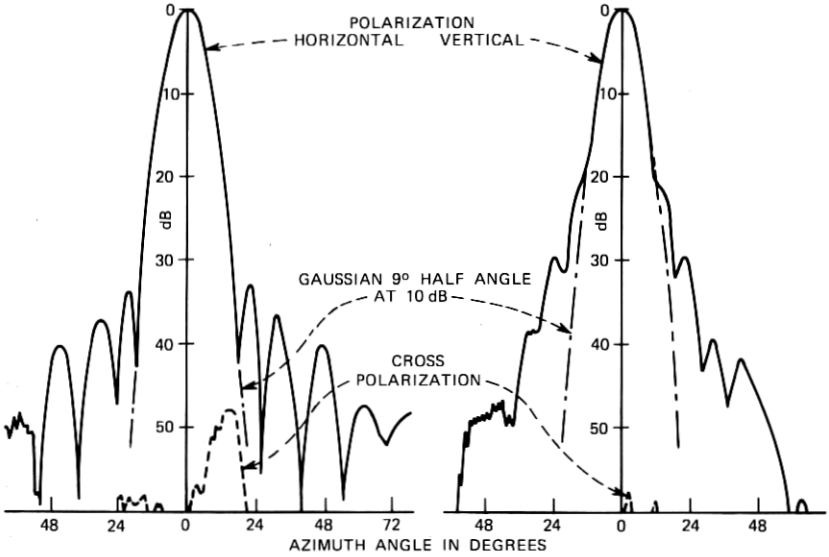

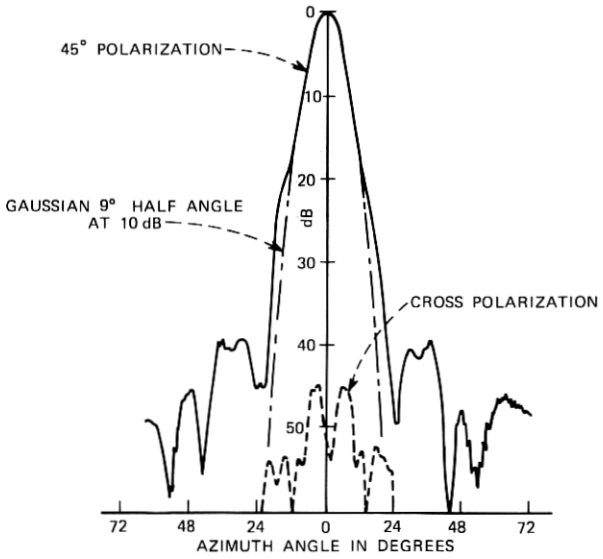

(b)

Fig. 3 (continued).

mode horns.) One can also see that, even though the quarter-wavelength aperture error fills in the first null in the feed-horn pattern, a shoulder appears at about −20 dB relative to the on-axis value for the case of horizontal polarization. At least 30 degrees of the feed pattern illuminates the reflector of the launcher (resulting in about

a 20-dB taper at the edge of the reflector in the principal polarization). Thus, the cross-polarization maxima in Fig. 3a also illuminate the reflector. However, as shown in Fig. 3b, when a grid polarizer is used on the dual-mode feed horn, the cross polarization for the 45-degree condition is reduced to a very acceptable −45-dB level. Also, with a polarizer on the horn, cross polarization for polarization in the principal planes is essentially nonexistent. Since one of the main purposes of the experiment is to measure the cross polarization generated by the offset reflector, as discussed in the next section, the feed horn per se must therefore be devoid of cross-polarized components. For that reason, the feed horn was equipped with a polarizer (patterns of Fig. 3b) for all ensuing measurements.

The dot-dash curves in Fig. 3b show that the feed-horn pattern is well approximated down to about −20 dB by a gaussian beam [eqs. (8) and (9)]. The 10-dB half angle, θ_e, used in the gaussian beam approximation, is 9 degrees.

The radiation patterns for the 19-GHz dual-mode feed horn are essentially the same as in Fig. 3. Significant cross-polarization levels were also observed at this frequency, but, using the polarizer, the cross polarization is reduced to a very acceptable level ($\leqq -50$ dB).

2.2 Antenna measuring range

A profile of the antenna range used for measuring the offset launcher is shown in Fig. 2b. To determine the cross-polarization characteristics at the range, a gently tapered pyramidal horn with a 15- by 15-cm aperture equipped with a wire grid polarizer (to eliminate any cross polarization caused by the horn itself) was used as the source. A standard gain horn with a similar polarizer was used as the receiver on the antenna azimuth-elevation positioner. These measurements show the cross polarization introduced by the range to be very small; in the range of interest, i.e., within ±3 degrees of the axial direction, it is of the order −47 dB.

2.3 Offset launcher measurements

Figure 1 is a photograph of one of the offset reflectors, along with its supporting structure. The reflector is illuminated by a 28.5-GHz dual-mode feed fitted with an etched grid polarizer as discussed in Section 2.1.

At 28.5 GHz, the far-field patterns in the principal and 45-degree polarizations, along with the associated cross polarizations for the offset launcher fed by a dual-mode horn with polarizer, are as shown in Fig. 4. Note the shoulders rather than sidelobe structure for the co-polar patterns. Although the shoulders in the launcher pattern are

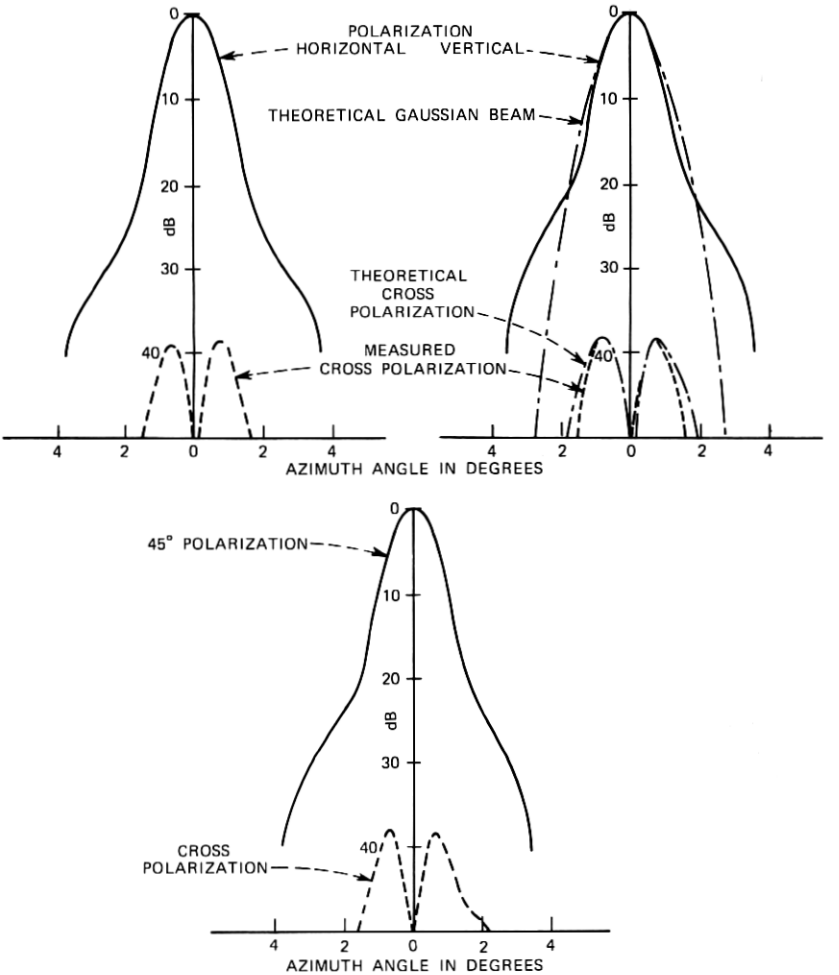

Fig. 4—Far-field radiation patterns of the principal and 45-degree planes for the offset launcher at 28.5 GHz with polarizer on horn. Theoretical (gaussian-beam) calculations are also included.

also apparent in the feed-horn patterns (compare the vertical polarization patterns of Figs. 3b and 4), this is not always the case. For example, the launcher pattern for horizontal polarization exhibits prominent shoulders (Fig. 4), whereas the corresponding feed-horn pattern (Fig. 3b) does not. Furthermore, the shoulders in the launcher patterns are at about the −24 dB level, while those in the feed-horn pattern are at about −20 dB. Most likely, the shoulders in the launcher patterns are due to the phase errors in the illumination which are caused by the finite taper length of the conical feed horn.

At 19.04 GHz, the co-polar and cross-polarization radiation patterns for the offset launcher are as shown in Fig. 5. Excellent symmetry is observed in the cross-polarization patterns even at this −40-dB level. Both Figs. 4 and 5 include the theoretical curves discussed in the next section.

One can see from the configuration of Fig. 1 that there is a possibility of a small amount of blockage by the feed and its mount (and subsequent cross-polarization effects) when the launcher is scanned upward in elevation. To examine this, a set of azimuth scans for various elevation settings was made at both 19.05 GHz and 28.5

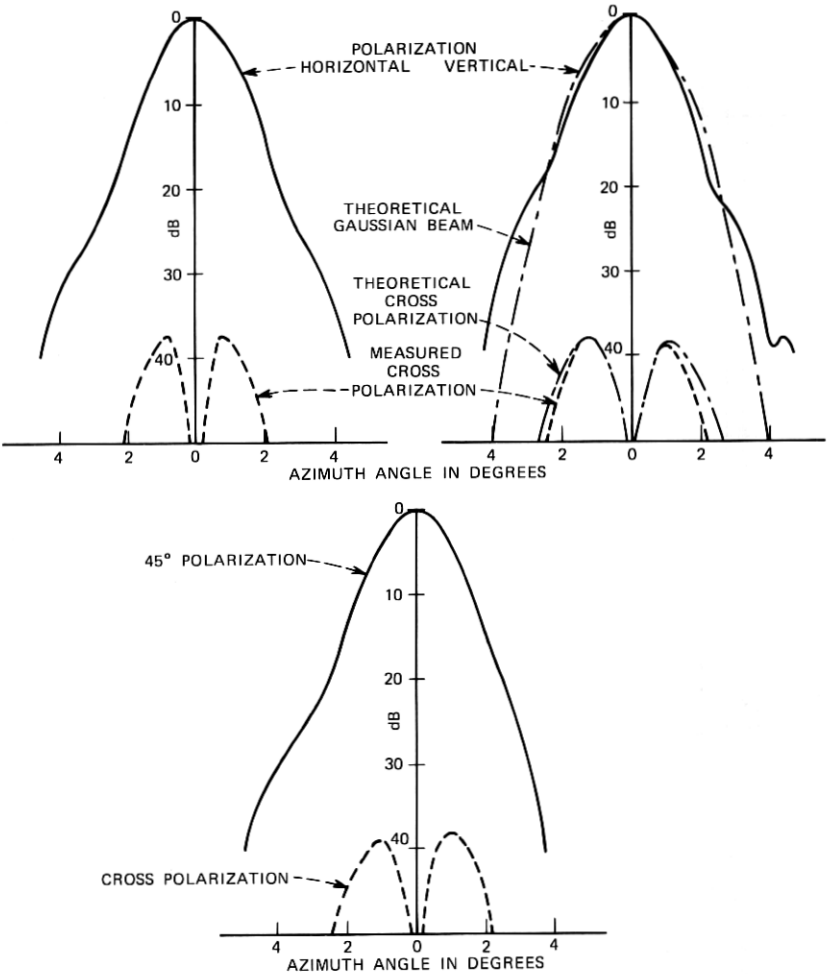

Fig. 5—Far-field radiation patterns of the principal and 45-degree planes for the offset launcher at 19.05 GHz. Dual-mode feed is equipped with polarizer on horn. Theoretical (gaussian-beam) calculations are also included.

GHz; the increase in cross polarization due to blockage was found to be negligible in both cases.

One may with justification raise the question as to why the cross polarization of the offset launcher, shown in Figs. 4 and 5, evidences values of the order of 38 dB even with a feed that has negligible cross polarization. There is an inherent depolarization introduced by an offset reflection surface,[2] which increases if θ_0, the angle between the feed axis and the reflector axis, is increased. Figure 6 shows the experimental results obtained by varying θ_0 between 12 and 26 degrees; the ratio of the maximum cross-polarized signal in the radiation pattern to the on-axis co-polarized signal correspondingly varies from −44 to −37 dB at both frequencies. Note that the ordinate of Fig. 6 is the average of the *peaks* of cross polarization obtained from an azimuth scan of the launcher; they should not be misinterpreted as on-axis values which, of course, are much lower. In the following section, we show that calculations based on gaussian-mode theory provide good agreement with the measured data; the theoretical result is shown by a solid curve in Fig. 6.

III. THEORY

3.1 Cross polarization in the aperture

An approximate method for computing the cross polarization due to the offset angle θ_0 consists of applying geometric optics to compute

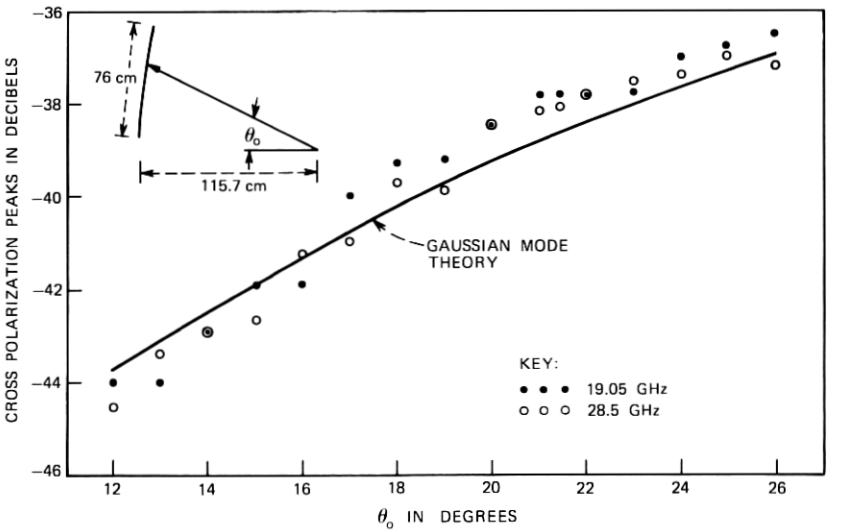

Fig. 6—Plot of cross-polarization peaks at 19.05 and 28.5 GHz introduced by the reflector itself as a function of offset angle, θ_0. Data are obtained by scanning the launcher in azimuth. Gaussian-mode theory is shown by the solid line. Incident polarization is horizontal.

the reflected field in the aperture from that radiated by the feed horn. The aperture field is then decomposed into two gaussian-beam modes to predict the far field of the offset launcher; this is a logical procedure because dual-mode horns produce an illumination that is approximated by a gaussian beam (see Fig. 3b).

The geometry of the offset launcher is shown in Fig. 7a. The dual-mode feed horn approximately provides "balanced feed" polarization[4] with respect to the coordinates (x', y', and z') aligned with the horn axis which is tilted at angle θ_0 from the reflector axis. The field radiated by the feed horn is given by

$$\mathbf{E}_{f'} = (\hat{\theta}' \sin \phi' + \hat{\phi}' \cos \phi') \frac{f'(\theta', \phi')}{r'}, \tag{1}$$

where $f'(\theta', \phi')$ is an arbitrary function of θ' and ϕ', and r', θ', and ϕ' are the usual spherical coordinates associated with the feed (see Fig. 7b). The caret indicates a unit vector. In eq. (1), the expressions corresponding to "vertical" polarization are used; identical results are obtained for "horizontal" polarization. ["Vertical" and "horizontal" are used in the sense that the polarization of the field in the aperture of an axisymmetric paraboloidal reflector coaxial with the feed-horn axis would be vertical or horizontal when the feed-horn polarization is as given in eq. (1).][5]

The axis of the paraboloidal reflector shown in Fig. 7a is co-linear with the $\hat{z}$ axis. An aperture field with no cross polarization would, therefore, result if the feed illumination were given by

$$\mathbf{E}_f = (\hat{\theta} \sin \phi + \hat{\phi} \cos \phi) \frac{f(\theta, \phi)}{r}, \tag{2}$$

where r, θ, and ϕ are the usual spherical coordinates associated with the x, y, z coordinates of Fig. 7a, i.e., the coordinates of a feed horn whose axis is aligned with the reflector axis. Theoretically, it is possible to hypothesize an asymmetric "balanced" feed whose axis is aligned with the reflector axis, giving the polarization of eq. (2), but whose amplitude distribution is offset to illuminate the reflector as would the amplitude distribution of a tilted symmetric "balanced" feed. Simple means (excluding multiple reflectors, etc.) are not known for the construction of such an asymmetric "balanced" feed. Therefore, in applications, one must approximate an asymmetric "balanced" feed horn with a tilted "balanced" feed horn; the cross polarization thereby introduced is calculated below.

Using geometric optics, we assert that if the polarization of a ray incident on the reflector from the feed is rotated by a given angle

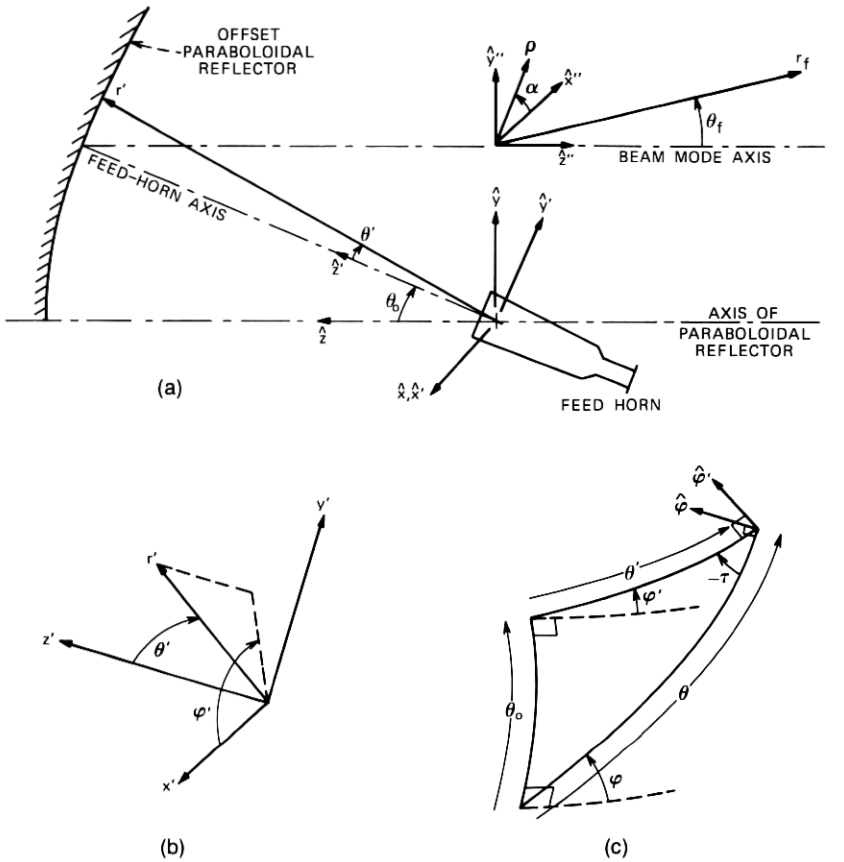

Fig. 7—(a) Launcher geometry. (b) Spherical coordinates. (c) Spherical triangle.

around the ray vector, then the polarization of the field of the corresponding ray in the reflector aperture is rotated by that same angle. By geometric optics, the intensity of the field in the aperture along a ray is the same as the intensity of the field incident on the reflector from the feed at its focus. Thus, the cross polarization in the aperture relative to the peak in-line polarization in the aperture can be computed by projecting the field of a tilted "balanced" feed horn, incident at any point on the reflector, onto the cross-polarized asymmetric "balanced" field at the same point and dividing by the peak in-line field of the tilted "balanced" feed horn; i.e.,

$$C(\theta', \phi') = \frac{\mathbf{E}_{f'} \cdot [\hat{\theta}(-\cos\phi) + \hat{\phi}\sin\phi]}{\mathbf{E}_{f'} \cdot [\hat{\theta}\sin\phi + \hat{\phi}\cos\phi]|_{\text{peak}}}. \tag{3}$$

Performing the scalar products indicated in eq. (3) yields

$$C(\theta', \phi') = \sin(\phi - \phi' + \tau)\frac{f'(\theta', \phi')}{r'} \cdot \left[\cos(\phi - \phi' + \tau)\frac{f'(\theta', \phi')}{r'}\bigg|_{\text{peak}}\right]^{-1}, \quad (4)$$

where τ is the angle between the primed and unprimed spherical angle coordinates shown in Fig. 7c. The angle, $\phi' - \phi - \tau$, is equal to the area, A (called spherical excess), of the spherical triangle shown in Fig. 7c and is related to the offset angle, θ_0, and the primed (feed horn) coordinates by the formula[6]

$$A = \phi' - \phi - \tau = 2\arctan\left[\frac{\cos\left(\frac{\theta_0 - \theta'}{2}\right)}{\left(\frac{\theta_0 + \theta'}{2}\right)}\cos\left(\frac{\phi'}{2} + \frac{\pi}{4}\right)\right] + \phi' - \frac{\pi}{2}. \quad (5)$$

The feed-horn amplitude pattern, f', is approximately uniform in ϕ' and maximum on axis (as for a corrugated or a dual-mode feed horn), and r', the distance from the feed to the reflector, is relatively constant over the region in which the cross-polarized field is a significant fraction of the peak in-line field. In this case, the cross-polarization amplitude can be approximated by

$$C(\theta', \phi') \doteq -\sin A\frac{f'(\theta')}{f'(0)}. \quad (6)$$

For a given θ', the ϕ' which maximizes A and the cross polarization is

$$\phi'_m = \arcsin\left(\tan\frac{\theta_0}{2}\tan\frac{\theta'}{2}\right). \quad (7)$$

For offset angles, θ_0, less than or equal to 90 degrees and θ' less than 30 degrees, which covers the case of interest, ϕ'_m is less than 16 degrees. This leads us to approximate ϕ'_m by 0 degrees, which results in a particularly simple yet accurate formula for the peak cross-polarization amplitude ratio, **C**, as will be shown. **C** is the ratio of the maximum cross-polarized amplitude to the maximum in-line polarized amplitude.

For dual-mode and corrugated horns, the pattern is approximated by a gaussian beam,[7]

$$f'(\theta') = e^{-a\theta'^2}, \quad (8)$$

where a is related to the 10-dB half-angle beamwidth, θ_c, by

$$a = \frac{\ln 10}{2\theta_c^2}. \quad (9)$$

Approximating ϕ_m' by 0 degrees, we have the following relation[6] for a right spherical triangle (Fig. 7c):

$$\sin A = \frac{\sin \theta_0 \sin \theta'}{1 + \cos \theta_0 \cos \theta'}. \tag{10}$$

Since we are interested in small θ',

$$\sin A = \frac{\theta' \sin \theta_0}{1 + \cos \theta_0}, \tag{11}$$

and eq. (6) becomes

$$C(\theta', \phi_m) \doteq - \frac{\sin \theta_0}{1 + \cos \theta_0} \theta' e^{-a\theta'^2}. \tag{12}$$

By differentiating eq. (12) to locate the angle which maximizes $C(\theta', \phi_m')$, we find

$$\theta_m' \doteq \sqrt{\frac{1}{2a}} = \theta_c / \sqrt{\ln 10}, \tag{13}$$

and

$$\mathbf{C}_a \doteq - \frac{\theta_c \tan \frac{\theta_0}{2}}{\sqrt{e \ln 10}}. \tag{14}$$

As mentioned above, **C** is the ratio of the maximum cross-polarized amplitude to the maximum in-line polarized amplitude. The subscript a indicates that the ratio is of the maxima found in the reflector aperture. If we denote by θ_T the half-angle of the gaussian beam approximation to the feed-horn pattern, where the power is T dB below that on axis, then eq. (14) becomes

$$\mathbf{C}_a \doteq - \theta_T \tan \frac{\theta_0}{2} \sqrt{\frac{10}{eT \ln 10}}. \tag{15}$$

By comparing eq. (14) with the exact formula for gaussian beams, eqs. (6), (7), and (8), eq. (14) is found accurate to within 0.1 dB for all offset angles, θ_0, less than or equal to 90 degrees and all 10-dB half-beamwidth angles, θ_c, less than or equal to 45 degrees. The maximum value of C in the exact formula was found by trial and error with the aid of a calculator.

The above calculations give the cross polarization in the reflector aperture; as will be shown in the next section, eq. (14) is also a good approximation for the far field in most cases.

3.2 Two-mode approximation to the aperture field

After reflection from the offset reflector, the gaussian beam from the horn is converted into two gaussian beam modes in the aperture:

a fundamental mode with the in-line polarization (denoted $\mathbf{E}_{00}$) and a higher-order gaussian beam mode which includes the cross polarization (denoted $\mathbf{E}_{01}$). Depending on the polarization of the feed horn, the polarization of the fundamental and higher-order modes vary as shown in Fig. 8. For an arbitrary balanced feed polarization, a superposition of the two polarization cases shown in Fig. 8 can be made.

The expressions for the gaussian beam modes are[7]

(*i*) Fundamental mode:

$$\mathbf{E}_{00} = (H_{00}\hat{x}'' + V_{00}\hat{y}'')\frac{\mathbf{w}_{00}}{w_{00}} \exp\left\{-jkz'' - \frac{\rho^2}{w_{00}^2} + j\left[\arctan\left(\frac{2z''}{k\mathbf{w}_{00}^2}\right) - \frac{k\rho^2}{2R_{00}}\right]\right\}, \quad (16)$$

(*ii*) Higher-order mode:

$$\mathbf{E}_{01} = |V_{01}(\hat{x}'' \cos\alpha - \hat{y}'' \sin\alpha) - H_{01}(\hat{x}'' \sin\alpha + \hat{y}'' \cos\alpha)|\frac{\sqrt{2}\rho\mathbf{w}_{01}}{w_{01}^2} \cdot \exp\left\{-jkz'' - \frac{\rho^2}{w_{01}^2} + j\left[2\arctan\left(\frac{2z''}{k\mathbf{w}_{01}^2}\right) - \frac{k\rho^2}{2R_{01}}\right]\right\}. \quad (17)$$

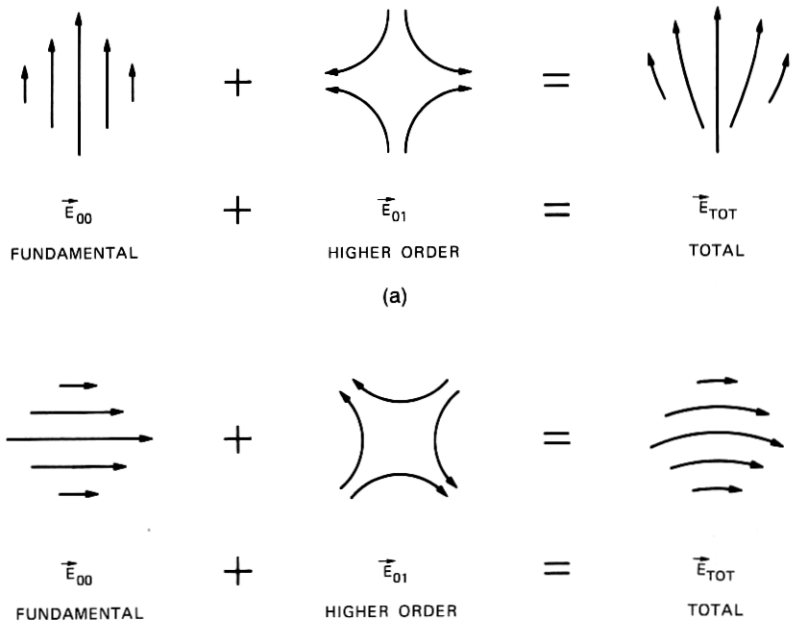

Fig. 8—Two-mode decomposition of aperture field (polarization looking in positive z direction, i.e., looking at the reflector). (a) Feed horn vertically polarized. (b) Feed horn horizontally polarized.

H_{00}, V_{00} and H_{01}, V_{01} are the phasor coefficients for horizontally and vertically polarized feeds. The subscripts refer to the standard TEM_{00} and TEM_{01} mode notations of Ref. 8; ρ, α, and z'' are cylindrical coordinates, with z'' denoting the distance along the beam axis from the beam waist. At the beam waist, the radius of curvature of the phase front, R, is infinite, and the field varies with increasing distance, ρ, from the axis at a rate determined by $\mathbf{w}$. For the fundamental mode, the field decreases to the $1/e$ value at $\rho = \mathbf{w}_{00}$. For the higher-order mode the field is maximum at $\rho = \mathbf{w}_{01}/\sqrt{2}$ and decreases to $\sqrt{2/e}$ of that value at $\rho = \mathbf{w}_{01}$. Away from the beam waist, $z'' \neq 0$, the field amplitude varies with ρ at a rate determined by w instead of $\mathbf{w}$, and the phase front has a finite radius of curvature, R. w and R are given by[8]

$$w = \mathbf{w}\sqrt{1 + \left(\frac{2z''}{k\mathbf{w}^2}\right)^2}, \tag{18}$$

and

$$R = z''\left[1 + \left(\frac{k\mathbf{w}^2}{2z''}\right)^2\right]. \tag{19}$$

Both modes have a characteristic exponential attenuation with distance from axis, $e^{-\rho^2/w^2}$, and a spherical wave front near the axis at constant z'', denoted by the term, $e^{-jk\rho^2/2R}$. Passing through a beam waist, the on-axis phase advances by π for the fundamental mode and 2π for the higher-order mode (relative to the plane-wave retardation, $e^{-jkz''}$). Thus, if the cross polarization and the in-line polarization are in phase at the beam waist (normally near the reflector aperture), they will be in phase quadrature at large distances from the beam waist (the far field). This phase quadrature relation gives rise to a beam shift with circular polarization as described in Ref. 2.

The choice of eq. (17) as the appropriate higher-order mode is based on its ability to approximate simultaneously both the cross polarization and the "space" taper (amplitude asymmetry from top to bottom of dish) of offset reflectors.

The in-line and cross-polarized fields in the aperture of the offset launcher of Fig. 1 were computed exactly by means of eq. (3); the resulting field-amplitude contours are shown in Fig. 9. In the aperture plane, the in-line and cross-polarized fields are in phase. Thus, the corresponding gaussian beam modes have their beam waists at the aperture and are in phase. This implies that the total field is linearly polarized everywhere in the aperture, and the direction of polarization varies in a manner determined by the ratio of the in-line and cross-polarized fields.

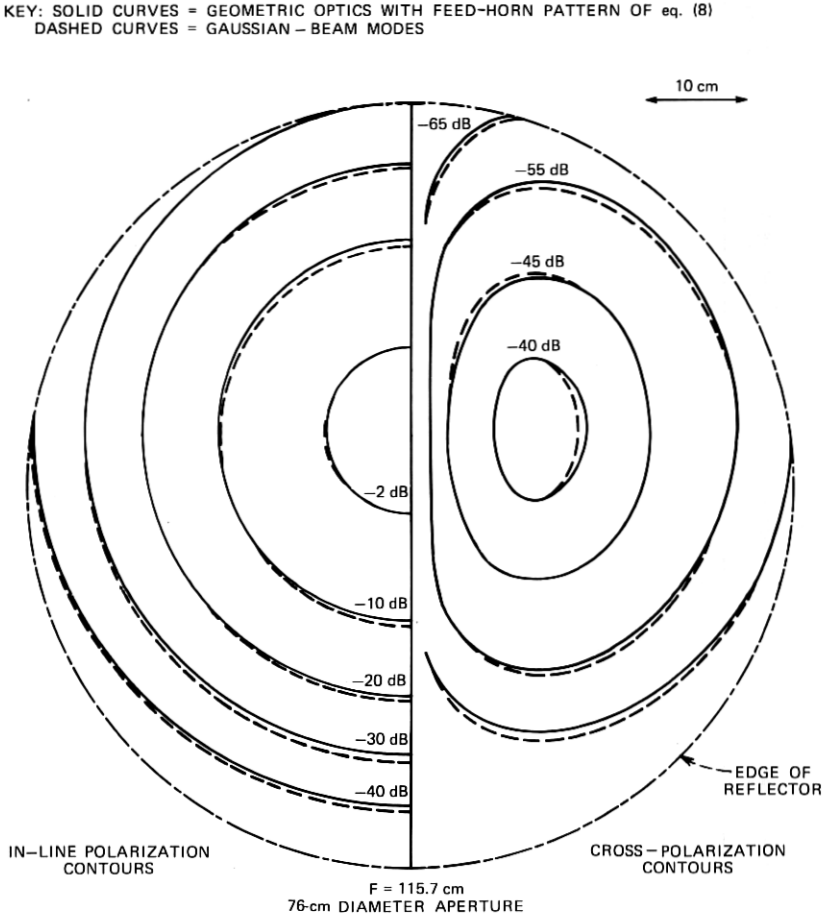

Fig. 9—Amplitude contours for the example reflector shown in Fig. 1.

The gaussian beam fields required to match the exactly computed aperture fields are found by first choosing a fundamental mode centered on the aperture with beam waist radius $\mathbf{w}_{00}$ such that it decreases 8.686 dB in power at the same radius as does the computed in-line polarized field, both being normalized to unit amplitude on axis.

With these criteria and the approximation that r' is nearly constant over the reflector,

$$r' \doteq r_0 = F \sec^2\left(\frac{\theta_0}{2}\right), \tag{20}$$

the parameters of the fundamental mode are determined as follows. The radius, $\rho_{1/e}$, at which the field drops to $1/e$ times its on-axis value

is found in the direction $\alpha = 0$. (Note that $\rho_{1/e}$ is larger in the $\alpha = -\pi/2$ direction and smaller in the $\alpha = \pi/2$ direction due to the space taper in these directions. Thus, $\rho_{1/e}$, as determined from the $\alpha = 0$ direction, approximates the average $\rho_{1/e}$ over all directions.)

$$\mathbf{w}_{00} \triangleq \rho_{1/e} = 2r_0 \sin\left(\tfrac{1}{2}\theta'_{1/e}\right), \tag{21}$$

where, from the gaussian approximation for the feed-horn pattern,

$$\theta'_{1/e} = \theta_c \sqrt{\frac{2}{\ln 10}}. \tag{22}$$

For unit amplitude on-axis, eq. (16) requires (we restrict our discussion here to the vertically polarized case; the horizontally polarized case yields identical expressions)

$$V_{00} = 1. \tag{23}$$

The higher-order mode parameters are found from the cross-polarization characteristics. Since the cross polarization is maximum at θ'_m, we have, from eq. (13),

$$\mathbf{w}_{01} = 2\sqrt{2}r_0 \sin\left(\tfrac{1}{2}\theta'_m\right) = 2\sqrt{2}r_0 \sin\left(\frac{\theta_c}{2\sqrt{\ln 10}}\right). \tag{24}$$

By comparing eqs. (24) and (21), it is seen that, for small θ_c, $\mathbf{w}_{01} \doteq \mathbf{w}_{00}$.

The amplitude of the higher-order gaussian beam mode is given by the maximum cross-polarization amplitude ratio ($\mathbf{C}_a$). From eqs. (14) and (17):

$$V_{01} = \frac{\theta_c \tan \dfrac{\theta_0}{2}}{\sqrt{\ln 10}}. \tag{25}$$

The phase of the higher-order mode follows from the fact that at the beam waist the in-line and cross-polarized fields are in phase.

Using eqs. (21) through (25), the gaussian beam mode approximations to the aperture fields, plotted as dashed contours in Fig. 9, compare favorably with those obtained by geometrical optics (solid contours).

3.3 The far fields

The parameters of the gaussian beam modes being thus determined, it is possible to compute the in-line and cross-polarized fields at any position in the main beam of the field radiated from the reflector. The far field is of particular interest,

$$z'' \gg \frac{k\mathbf{w}^2}{2}, \tag{26}$$

allowing eqs. (18) and (19) to be approximated by

$$w \doteq \frac{2z''}{k\mathbf{w}} \quad \text{and} \quad R \doteq z''. \tag{27}$$

Also, if the beamwidth is small,

$$r_f \doteq \sqrt{(z'')^2 + \rho^2} = z'' + \frac{\rho^2}{2z''}; \quad \theta_f \doteq \frac{\rho}{z''}. \tag{28}$$

From eqs. (16) and (17), the in-line field is therefore given by

$$E_V \doteq \frac{jke^{-jkr_f}}{2r_f}\left[V_{00}\mathbf{w}_{00}^2 \exp\left(-\frac{\theta_f^2}{\psi_{00}^2}\right) - j\sqrt{2}V_{01}\mathbf{w}_{01}^2 \frac{\theta_f}{\psi_{01}} (\sin\alpha) \exp\left(-\frac{\theta_f^2}{\psi_{01}^2}\right)\right] \tag{29}$$

and the cross-polarized field by

$$E_H = -\frac{ke^{-jkr_f}}{2r_f}\sqrt{2}V_{01}\mathbf{w}_{01}^2 \frac{\theta_f}{\psi_{01}} (\cos\alpha) \exp\left(-\frac{\theta_f^2}{\psi_{01}^2}\right), \tag{30}$$

for the "vertically" polarized feed. We have defined

$$\psi_{00} \triangleq \frac{2}{k\mathbf{w}_{00}} \quad \text{and} \quad \psi_{01} \triangleq \frac{2}{k\mathbf{w}_{01}}, \tag{31}$$

the angular beam radii in the far field.

The $\mathbf{C}_f$ from eqs. (14), (23), (25), (29), and (30), where the subscript, f, indicates the far-field maximum cross-polarization amplitude ratio, is

$$\mathbf{C}_f = j\frac{V_{01}}{V_{00}\sqrt{e}}\left(\frac{\mathbf{w}_{01}}{\mathbf{w}_{00}}\right)^2 = \mathbf{C}_a\left(\frac{\mathbf{w}_{01}}{\mathbf{w}_{00}}\right)^2. \tag{32}$$

Thus, the far-field $\mathbf{C}$ is $j(\mathbf{w}_{01}/\mathbf{w}_{00})^2$ times that in the aperture and occurs in the azimuth plane at an angle

$$\frac{\psi_{01}}{\sqrt{2}} = \frac{\sqrt{2}}{k\mathbf{w}_{01}} \text{ radians.} \tag{33}$$

As mentioned above, for small feed beamwidths, θ_c,

$$\mathbf{w}_{01} \doteq \mathbf{w}_{00}, \tag{34}$$

so the far-field $\mathbf{C}$ is approximately equal to that of the aperture, and the peak cross-polarization lobe occurs at approximately the -4.34-dB level of the main beam.

A comparison of the experimental and theoretical far-field patterns for in-line and cross-polarized fields from the offset launcher of Fig. 1 at 28.56 GHz and 19.04 GHz are shown in Figs. 4 and 5. The main discrepancy between theory and experiment are the shoulders on the

sides of the experimental pattern at a level of about −24 dB not present on the sides of the theoretical main beam. As mentioned in Section 2.3, the shoulders are probably due to phase error in the horn aperture which is not in the gaussian feed pattern assumed in the theory.

3.4 Truncation effects

The effect of truncating the aperture of the launcher at various circular contours of the fundamental mode can be computed. Let the radius of the aperture at the truncation be c. Then the taper at the truncation is

$$T = \left(\frac{20}{\ln 10}\right)\left(\frac{c}{\mathbf{w}_{00}}\right)^2. \tag{35}$$

The radiation integrals in the x'', z'' plane (where the cross-polarization is largest) for the fundamental mode and higher-order mode are

$$E_{00_f} = \int_0^c \rho d\rho \int_0^{2\pi} d\alpha V_{00} \exp\left[-\left(\frac{\rho}{\mathbf{w}_{00}}\right)^2 - jk\rho \cos\alpha \sin\theta_f\right], \tag{36}$$

and

$$E_{01_f} = -\int_0^c \rho d\rho \int_0^{2\pi} d\alpha V_{01} \frac{\sqrt{2}\rho}{\mathbf{w}_{01}} \cdot \exp\left[-\left(\frac{\rho}{\mathbf{w}_{01}}\right)^2 - jk\rho \cos\alpha \sin\theta_f\right] \cos\alpha \cos\theta_f. \tag{37}$$

From eq. (36), the in-line polarization far-field on-axis is

$$E_{00_f}(\theta_f = 0) = \pi V_{00}\mathbf{w}_{00}^2\left[1 - \exp\left(-\frac{c^2}{\mathbf{w}_{00}^2}\right)\right]. \tag{38}$$

The cross-polarized far-field pattern from (37) is, letting $\cos\theta_f \doteq 1$,

$$E_{01_f} \doteq \frac{j\pi V_{01}\mathbf{w}_{01}^2}{\sqrt{e}} I(\theta_f), \tag{39}$$

where

$$I(\theta_f) \triangleq 2\sqrt{2e}\int_0^{c/\mathbf{w}_{01}} t^2 e^{-t^2} J_1(tk\mathbf{w}_{01} \sin\theta_f) dt, \tag{40}$$

and $J_1(x)$ is the first-order Bessel function of the first kind. From eqs. (34) and (35), choosing the taper, T, determines $I(\theta_f)$. Numerically integrating eq. (40), the peak value, I_P, of $I(\theta_f)$ and the location, θ_{f_p}, at which $I(\theta_f)$ is maximum were determined for various tapers, T. The resulting far field $\mathbf{C}_f$ relative to that of an infinite aperture,

$$-20 \log_{10}\left(\frac{\mathbf{C}_f}{\mathbf{C}_{f\infty}}\right) = -20 \log_{10}\left(\frac{I_P}{1 - e^{-c^2/\mathbf{w}200}}\right), \tag{41}$$

is plotted in Fig. 10 along with the angular position, θ_{fP}, of the peak in the cross-polarization lobe relative to that, $\theta_{fp\infty}$, of an infinite aperture. Notice that the effect of truncation is to reduce the cross-polarized signal relative to the co-polarized signal (higher $\mathbf{C}_f$) and to move the cross-polarization lobes out to larger angles off-axis. Furthermore, these truncation effects depend only on the truncation taper and are essentially independent of the offset geometry.

Figure 11 shows $\mathbf{C}_f$ as determined from the gaussian beam formulas for a wide range of offset reflector geometries indicating an infinite aperture (no truncation) and the aperture truncated at a 10-dB taper. With the infinite aperture, the $\mathbf{C}_f$ from the gaussian beam theory are within 0.2 dB of the cross polarization in the aperture, $\mathbf{C}_a$ (not shown), for all geometries on the figure. When the aperture is truncated at the 10-dB level, $\mathbf{C}_f$ is, from Fig. 10, 2.2 dB smaller than that for the infinite aperture, as is also seen from the dashed curve in Fig. 11. These dashed curves agree with cross polarization obtained by numerically computing[2] the radiation integral over the aperture field found by geometrical optics projection of the radiation pattern of a dual-mode feed horn.

Using eqs. (14) and (32), the maximum cross-polarization levels as a function of offset angle were computed for the precise geometry

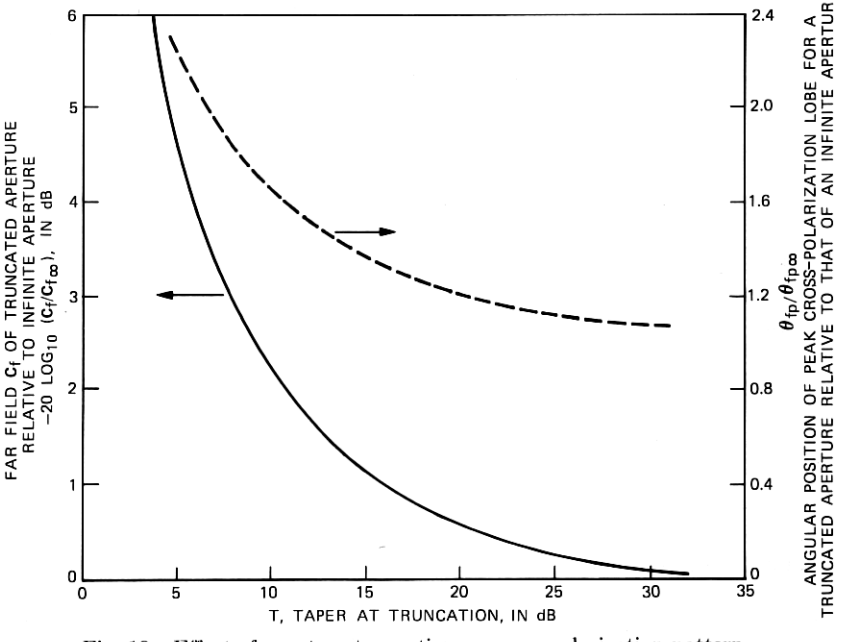

Fig. 10—Effect of aperture truncation on cross-polarization pattern.

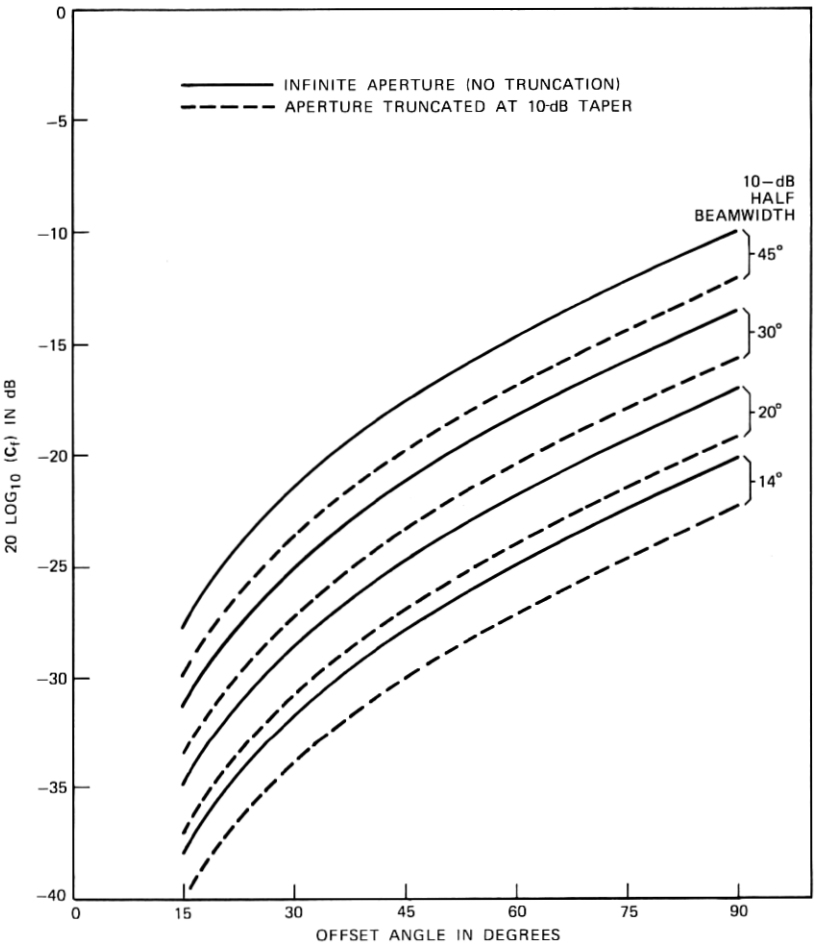

Fig. 11—Maximum cross-polarization amplitude ratio for a range of offset geometries.

of the offset launcher of Fig. 1. The factor $(w_{01}/w_{00})^2$ which converts aperture cross polarization to far-field cross polarization is only 1.0004 (i.e., 0.008 dB). The 10-dB half angle, θ_c, of the feed-horn gaussian-beam approximation (discussed in Section 2.1) is 9 degrees. The calculated cross polarization is compared with the measured cross polarization as a function of offset angle in Fig. 6. The theory appears to be in good agreement with the measurements at both frequencies.

IV. CONCLUSIONS

It has been demonstrated that an offset launcher can provide low cross polarization and a low-sidelobe symmetrical beam when fed

with a suitable horn at a small enough offset angle. Simple formulas for the far-field performance of the launcher are derived in terms of two gaussian modes; comparison with measurements at 19 and 28 GHz shows good agreement. The maximum cross-polarization amplitude ratio is found to change little from aperture to far field. Offset reflector geometries have also been useful for multiple-beam applications.[9,10]

V. ACKNOWLEDGMENTS

It is a pleasure to acknowledge D. C. Hogg for many helpful suggestions, and W. E. Legg and R. H. Turrin for measurements of the dual-mode feed horn.

REFERENCES

1. C. Dragone and D. C. Hogg, "The Radiation Pattern and Impedance of Offset and Symmetrical Near-Field Cassegrainian and Gregorian Antennas," IEEE Trans. Antennas & Propagation, *AP-22*, No. 3 (May 1974), p. 472.
2. T. S. Chu and R. H. Turrin, "Depolarization Properties of Offset Reflector Mirrors," IEEE Trans. Microwave Theory & Techniques, *MTT-23*, No. 4 (April 1975), pp. 377–379.
3. J. A. Arnaud and J. T. Ruscio, "Guidance of 100-GHz Beams by Cylindrical Mirrors," IEEE Trans. Microwave Theory & Techniques, *MTT-23*, No. 4 (April 1975), pp. 377–379.
4. R. H. Turrin, "Dual Mode Small-Aperture Antennas," IEEE Trans. Antennas & Propagation, *AP-15*, No. 2 (March 1967), pp. 307–308.
5. E. M. T. Jones, "Paraboloid Reflector and Hyperboloid Lens Antennas," IRE Trans. Antennas and Propagation, *AP-2* (July 1954), pp. 119–127.
6. *Reference Data for Radio Engineers*, Fifth Edition, ITT, New York: H. W. Sams, 1968, pp. 44–9—44–10.
7. G. Gaubau and F. Schwering, "On the Guided Propagation of Electromagnetic Wave Beams," IRE Trans. Antennas & Propagation, *AP-9*, No. 3 (May 1961), pp. 248–256.
8. H. Kogelnik and T. Li, "Laser Beams and Resonators," Applied Optics, *5*, No. 10 (October 1966), pp. 1550–1567.
9. C. J. Sletten et al., "Corrective Line Sources for Paraboloids," IRE Trans. Antennas & Propagation, *AP-6* (July 1958), pp. 239–251.
10. E. A. Ohm, "A Proposed Multiple-Beam Microwave Antenna for Earth Stations and Satellites," B.S.T.J., *53*, No. 8 (October 1974), pp. 1657–1667.